Exact amplitudes of six polarization modes for gravitational waves

Young-Hwan Hyun*
Korea Institute of Science and Technology Information (KISTI), 245 Daehak-ro, Yuseong-gu, Daejeon 34141, Republic of Korea

Yoonbai Kim† and Seokcheon Lee‡
Department of Physics and Institute of Basic Science, Sungkyunkwan University, Suwon 16419, Republic of Korea

(Received 20 March 2019; published 10 June 2019)

The exact amplitudes of six polarization modes of gravitational waves are constructed in terms of both the small metric perturbations and the Newman-Penrose scalars. The obtained formulas are applicable to any metric-compatible gravity theories whose gravitational waves propagate along either the null or non-null geodesics. Once a gravity theory (specifically, its linearized wave equation) is written, comparison to the observed data of the laser interferometer experiments is direct.

DOI: 10.1103/PhysRevD.99.124002

I. INTRODUCTION

To date, Einstein's general relativity (GR) has passed all experimental tests, and thus it is important to ensure that extensions of gravity also pass these same tests. Such longevity is not only related to its absolute correctness, but can also motivate more accurate tests to probe the corrections to Einstein's GR. New precession searches for small deviations from GR are intriguing in the context of astrophysics and cosmology. The first candidate experiment for identifying violations of GR is to look for the possible polarization modes of gravitational waves (GWs), and its formulation was first constructed in Refs. [1,2] (see also the reviews [3,4]).

Einstein's GR predicted the existence of gravitational waves [5], and the long-awaited signal of gravitational waves was picked up by the Advanced Laser Interferometer Gravitational-wave Observatory (aLIGO) and Virgo collaborations [6–9]. This milestone in gravitational-wave research opens a window to probe the highly dynamical and strong-field regimes of gravity [10,11]. In addition, aLIGO and Virgo also allow for the precision study of the polarization modes of gravitational waves, particularly the bound of the nontensorial modes [12,13]. Analyses of known galactic pulsars have constrained the strain of the scalar and vector modes to be below 1.5×10^{-26} at 95% credibility [12], which is the first direct upper limit for a nontensorial strain. This upper bound provides a guideline to modify the beyond-GR theories of gravity.

In the context of metric-compatible theories, there are six polarization modes: the breathing (b), longitudinal (l), vector-x (x), vector-y (y), plus ($+$), and cross ($\times$) modes. Einstein's GR predicts transverse and traceless waves whose quantization leads to massless spin-2 gravitons, and thus the detection of only the two tensor modes (plus and cross polarization modes) will fulfill GR's prediction. The six polarization modes of gravitational waves have been studied under the assumption of weak, plane, and null propagation and analyzed in terms of the Newman-Penrose (NP) formalism [1]. Most of the subsequent research on various extended models of gravity has employed this formalism with the E(2) classification to calculate the NP scalars corresponding to each polarization mode [10, 14–16], even for theories involving massive modes [10,17–24]. In the case of the bimetric theory, NP scalars have been used to show how massive degrees of freedom (d.o.f.) contribute to the amplitude of nontensorial modes [20,25]. This is because the NP scalars provide the simplest way to look at a specific propagation of gravitational waves even in extended gravity theories; however, the NP analysis in Ref. [1] is no longer exact for the massive gravity theories. Therefore, it is necessary to construct the exact formalism for the six polarization modes of the non-null propagating gravitational waves. Recently, this point was indicated in Ref. [26]. There have also been developments in numerical simulations for the modification of Newtonian gravity by including a Yukawa-type potential [27–29].

It is timely to reconstruct the formalism to give a correct interpretation of the non-null propagation seen in the observed gravitational-wave data. In this work, we obtain the formulas for the six polarization amplitudes connecting the observed data from the laser interferometers and the

*younghwan.hyun@gmail.com
†yoonbai@skku.edu
‡skylee2@gmail.com

GWs of the proposed gravity theory. These are also applicable to the non-null propagation of GWs. Let us begin by introducing the assumptions of our formalism:

(1) The gravity theories we consider are metric compatible.

(2) The amplitude of the perturbation is small and the characteristic length scale is much smaller than that of the background curvature. This is the so-called short-wavelength approximation.

The aforementioned assumptions dictate the following guidelines:

(1) Since any metric-compatible theory is allowed, the geodesic equation and the Bianchi identity can be used. On the other hand, the specific form of the action (e.g., the Einstein-Hilbert action for GR) or, equivalently, the corresponding dynamical equations (e.g., the Einstein equations) need not be assumed in a derivation of the formalism. In practice, this means that any metric-compatible gravity action [which can involve not only GR but also many other candidate theories, e.g., higher-derivative, $f(R)$, or massive gravity theories] can utilize our formalism without restriction.

(2) The linear wave equations for the weak gravitation field $h_{\mu\nu}$ allow us to determine the physical contents of the GWs through the dispersion relation $\omega = \omega(\boldsymbol{k})$ and their six polarization modes.

The six polarization modes are formulated in terms of both the NP scalars and the six physical degrees of freedom among the ten components of $h_{\mu\nu}$ by appropriate gauge fixing. Since the formalism is written in terms of the detector response function, a comparison between the theory (say, the action) and the observed data can directly be performed.

This work is organized as follows. In Sec. II, we review the formalism of Ref. [1]. In Sec. III A, we describe the six polarization modes based on the usual NP formalism. We express the exact driving-force matrix for the plane-wave weak propagations of gravitational waves based on the NP formalism in Sec. III B and in terms of the metric perturbations in Sec. III C. A discussion on the difference between the usual and exact results is also included. In Sec. III D, we obtain the response functions. Some known gravity models are analyzed in Sec. IV and the Appendix. We conclude in Sec. V with a few research directions.

II. SIX OBSERVABLES OF GRAVITATIONAL WAVES

When a freely falling observer is at a fiducial point in an approximately Lorentz normal coordinate system $(t, x^i) = (t, x, y, z)$, where x^i are the spatial coordinates of the test particle at rest, the acceleration relative to the location of the observer is depicted by the geodesic deviation equation [1],

$$a_i = -R_{0i0j}x^j, \tag{1}$$

where the electric components of the Riemann tensor R_{0i0j} (the so-called Riemann field) are the only measurable quantities in gravitational-wave detection. Suppose that a propagating gravitational wave is weak and a plane wave. When the z direction is chosen parallel to the propagation of gravitational waves, every component of the Riemann field $R_{0i0j}(t_{\mathrm{r}})$ becomes a function of a retarded time, $t_{\mathrm{r}} = t - z/v$.

The six electric components of the Riemann tensor are set by the symmetric driving-force matrix $S_{ij}(t)$ [1,30],

$$S_{ij}(t_{\mathrm{r}}) \equiv R_{0i0j}(t_{\mathrm{r}}). \tag{2}$$

Since this driving-force matrix possesses six independent d.o.f., the six basis polarization matrices are introduced as

$$E_1(\hat{z}) = \begin{pmatrix} 0 & 0 & 0 \\ 0 & 0 & 0 \\ 0 & 0 & 1 \end{pmatrix}, \quad E_2(\hat{z}) = \begin{pmatrix} 0 & 0 & 1 \\ 0 & 0 & 0 \\ 1 & 0 & 0 \end{pmatrix},$$
$$E_3(\hat{z}) = \begin{pmatrix} 0 & 0 & 0 \\ 0 & 0 & 1 \\ 0 & 1 & 0 \end{pmatrix}, \quad E_4(\hat{z}) = \frac{1}{2}\begin{pmatrix} 1 & 0 & 0 \\ 0 & -1 & 0 \\ 0 & 0 & 0 \end{pmatrix},$$
$$E_5(\hat{z}) = \begin{pmatrix} 0 & 1 & 0 \\ 1 & 0 & 0 \\ 0 & 0 & 0 \end{pmatrix}, \quad E_6(\hat{z}) = \frac{1}{2}\begin{pmatrix} 1 & 0 & 0 \\ 0 & 1 & 0 \\ 0 & 0 & 0 \end{pmatrix}. \tag{3}$$

Note that the coefficients in front of the matrices were set differently in Ref. [1] to read the polarization amplitudes in the NP formalism. In the basis of polarization matrices, the driving-force matrix is expanded in terms of the polarization amplitudes p_n,

$$S(t) = \sum_{A=1}^{6} p_A(\hat{z}, t) E_A(\hat{z}), \tag{4}$$

and a comparison of Eqs. (2) and (4) gives

$$S = \begin{pmatrix} R_{txtx} & R_{txty} & R_{txtz} \\ R_{tytx} & R_{tyty} & R_{tytz} \\ R_{tztx} & R_{tzty} & R_{tztz} \end{pmatrix} = \begin{pmatrix} \frac{1}{2}(p_4 + p_6) & p_5 & p_2 \\ p_5 & \frac{1}{2}(-p_4 + p_6) & p_3 \\ p_2 & p_3 & p_1 \end{pmatrix}. \tag{5}$$

Each polarization amplitude of the six electric components $p_1, \ldots, p_6$ corresponds to a specific geometrical distortion of the test-particle distribution, whose shapes are displayed in Fig. 1 (see Ref. [1]). The modes $p_1, \ldots, p_6$ are the longitudinal, vector-x, vector-y, plus, cross, and breathing polarization modes, respectively. Thus, in our basis (3), the

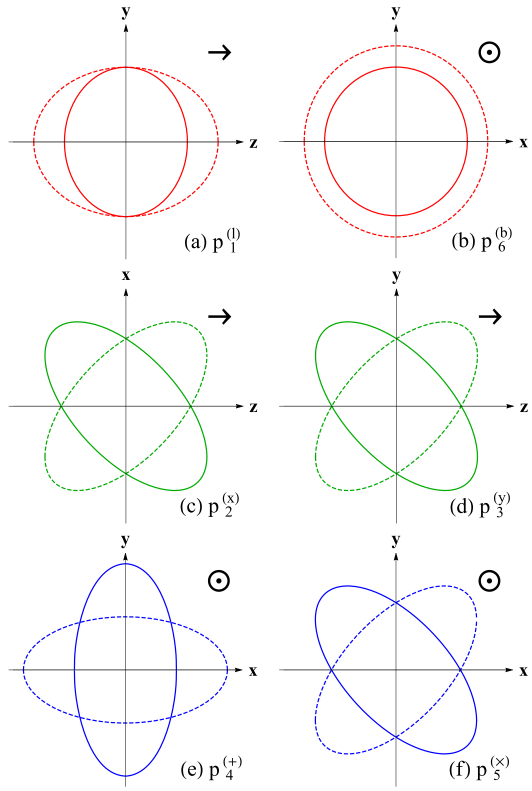

FIG. 1. The six polarization modes: (a) breathing mode $p_1^{(b)}$, (b) longitudinal mode $p_6^{(l)}$, (c) vector-x mode $p_2^{(x)}$, (d) vector-y mode $p_3^{(y)}$, (e) plus mode $p_4^{(+)}$, and (f) cross mode $p_5^{(\times)}$. Here we added the superscript of every corresponding polarization mode to p_n to clearly show its geometrical description. The red, green, and blue curves indicate scalar, vector, and tensor modes, respectively. The circled dot in panels (b), (e), and (f) indicates that the wave is propagating out of the page, and the right-pointing arrow in panels (a), (c), and (d) indicates that the wave is propagating in the z direction.

exact polarization amplitudes are written in terms of the driving-force matrix element in its simplest form,

$$\begin{aligned}
&p_1^{(l)} \equiv R_{tztz}, \qquad p_2^{(x)} \equiv R_{tztx}, \qquad p_3^{(y)} \equiv R_{tzty},\\
&p_4^{(+)} \equiv R_{txtx} - R_{tyty}, \qquad p_5^{(\times)} \equiv R_{txty},\\
&p_6^{(b)} \equiv R_{txtx} + R_{tyty},
\end{aligned} \tag{6}$$

where we add the description of the mode in the superscript for a clear distinction.

III. POLARIZATION MODES

A. Null propagation of gravitational waves

In this subsection, we briefly recapitulate the previous conventional method on the six polarization modes of the massless gravitons in which the null propagation assumption is adopted [1]. We will examine the amplitude expressions in the traditional NP method to find necessary corrections to extend the exact formalism to the massive gravitational waves following the non-null geodesic.

For the description of the polarization modes under the null propagation assumption, it is convenient to introduce the NP quantities for simplicity. For a local null tetrad basis k and two null spin tetrads m and $\bar{m}$, we have the four tetrad basis vectors,

$$\begin{aligned}
\boldsymbol{k} &= \frac{1}{\sqrt{2}}(\partial_t + \partial_z), \qquad \boldsymbol{l} = \frac{1}{\sqrt{2}}(\partial_t - \partial_z),\\
\boldsymbol{m} &= \frac{1}{\sqrt{2}}(\partial_x + i\partial_y), \qquad \bar{\boldsymbol{m}} = \frac{1}{\sqrt{2}}(\partial_x - i\partial_y),
\end{aligned} \tag{7}$$

which satisfy the normalization conditions

$$k_\mu l^\mu = -1, \qquad m_\mu \bar{m}^\mu = 1. \tag{8}$$

In four dimensions, the Riemann tensor is split into three irreducible parts—$C_{\mu\nu\rho\sigma}$, $R_{\mu\nu} - \frac{1}{4} g_{\mu\nu} R$, and R—where the Weyl tensor in the four-dimensional spacetime is defined by

$$\begin{aligned}
C_{\mu\nu\rho\sigma} &= R_{\mu\nu\rho\sigma} - (g_{\mu[\rho} R_{\sigma]_\nu} - g_{\nu[\rho} R_{\sigma]_\mu}) + \frac{1}{3} g_{\mu[\rho} g_{\sigma]\nu} R\\
&\equiv R_{\mu\nu\rho\sigma} - 2 g_{[\mu|[\rho} R_{\sigma]|\nu]} + \frac{1}{3} g_{\mu[\rho} g_{\sigma]\nu} R.
\end{aligned} \tag{9}$$

In the NP formalism, the five complex Weyl-NP scalars are defined and classified with spin weights from the Weyl tensor,

$$\begin{aligned}
&s = +2\colon\ \Psi_0 \equiv C_{kmkm},\\
&s = +1\colon\ \Psi_1 \equiv C_{klkm} = C_{\bar{m}mkm},\\
&s = 0\colon\ \Psi_2 \equiv C_{km\bar{m}l} = \frac{1}{2}(C_{klkl} + C_{klm\bar{m}}) = \frac{1}{2}(C_{\bar{m}m\bar{m}m} + C_{klm\bar{m}}),\\
&s = -1\colon\ \Psi_3 \equiv C_{kl\bar{m}l} = C_{\bar{m}m\bar{m}l},\\
&s = -2\colon\ \Psi_4 \equiv C_{\bar{m}l\bar{m}l}.
\end{aligned} \tag{10}$$

The ten Ricci-NP scalars are defined from the traceless and trace parts of the Ricci tensor $R_{\mu\nu}$ as

$$\begin{aligned}
&s = +2\colon\ \Phi_{02} \equiv \frac{1}{2} R_{mm},\\
&s = +1\colon\ \begin{cases} \Phi_{01} \equiv \frac{1}{2} R_{km},\\ \Phi_{12} \equiv \frac{1}{2} R_{lm}, \end{cases}\\
&s = 0\colon\ \begin{cases} \Phi_{00} \equiv \frac{1}{2} R_{kk},\\ \Phi_{11} \equiv \frac{1}{4}(R_{kl} + R_{m\bar{m}}),\\ \Phi_{22} \equiv \frac{1}{2} R_{ll}, \end{cases}\\
&s = -1\colon\ \begin{cases} \Phi_{10} \equiv \frac{1}{2} R_{k\bar{m}} = \Phi_{01}^*,\\ \Phi_{21} \equiv \frac{1}{2} R_{l\bar{m}} = \Phi_{12}^*, \end{cases}\\
&s = -2\colon\ \Phi_{20} \equiv \frac{1}{2} R_{\bar{m}\bar{m}} = \Phi_{02}^*,\\
&\Lambda \equiv \frac{R}{24} = \frac{1}{12}(R_{m\bar{m}} - R_{kl}).
\end{aligned} \tag{11}$$

Under the null condition the measurable field becomes a function of the retarded time $t_r = t - z$ with $v = 1$, and thus the Riemann tensor satisfies

$$R_{abcd,p} = 0, \tag{12}$$

where (a, b, c, d) range over $(k, l, m, \bar{m})$ and $(p, q, \cdots)$ only range over $(k, m, \bar{m})$. With the help of the Bianchi identity,

$$R_{ab[pq,l]} = \frac{1}{3}(R_{abpq,l} + R_{abql,p} + R_{ablp,q}) = \frac{1}{3}R_{abpq,l} = 0, \tag{13}$$

Eq. (12) leads to a constant curvature solution. Since any nonvanishing constant curvature solution is irrelevant for wave phenomena, only the solution of our interest should have a vanishing Riemann tensor component,

$$R_{abpq} = 0 = R_{pqab}. \tag{14}$$

Therefore, all nonvanishing components of the Riemann tensor should take the form R_{plql}. Accordingly, under the null condition, all of the NP scalars in Eqs. (10) and (11) are given by

$$\begin{aligned}
&\Psi_0 = C_{kmkm} = R_{kmkm} \overset{\text{null}}{\rightarrow} 0,\\
&\Psi_1 = C_{klkm} = R_{klkm} - \frac{1}{2}R_{km} \overset{\text{null}}{\rightarrow} 0,\\
&\Psi_2 = C_{km\bar{m}l} = R_{km\bar{m}l} - \frac{1}{12}R \overset{\text{null}}{\rightarrow} \frac{1}{6}R_{klkl},\\
&\Psi_3 = C_{kl\bar{m}l} = R_{kl\bar{m}l} - \frac{1}{2}R_{l\bar{m}} \overset{\text{null}}{\rightarrow} \frac{1}{2}R_{kl\bar{m}l},\\
&\Psi_4 = C_{\bar{m}l\bar{m}l} = R_{\bar{m}l\bar{m}l} \overset{\text{null}}{\rightarrow} R_{\bar{m}l\bar{m}l}, \qquad \Phi_{00} = \frac{1}{2}R_{kk} \overset{\text{null}}{\rightarrow} 0,\\
&\Phi_{01} = \Phi^*_{10} = \frac{1}{2}R_{km} \overset{\text{null}}{\rightarrow} 0,\\
&\Phi_{02} = \Phi^*_{20} = \frac{1}{2}R_{mm} \overset{\text{null}}{\rightarrow} 0,\\
&\Phi_{11} = \frac{1}{4}(R_{kl} + R_{m\bar{m}}) \overset{\text{null}}{\rightarrow} \frac{1}{4}R_{klkl} = \frac{3}{2}\Psi_2 (= \Psi_2 - \Lambda),\\
&\Phi_{12} = \Phi^*_{21} = \frac{1}{2}R_{lm} \overset{\text{null}}{\rightarrow} \frac{1}{2}R_{klml} = \Psi^*_3,\\
&\Phi_{22} = \frac{1}{2}R_{ll} = R_{ml\bar{m}l} \overset{\text{null}}{\rightarrow} R_{ml\bar{m}l},\\
&\Lambda = \frac{R}{24} = -\frac{1}{12}(R_{kl} - R_{m\bar{m}}) \overset{\text{null}}{\rightarrow} -\frac{1}{12}R_{klkl} = -\frac{1}{2}\Psi_2,
\end{aligned} \tag{15}$$

where $R = -2R_{kl} = -2R_{klkl}$ is used in the last formula. Eight of the 15 NP scalars do not vanish, but only four NP scalars, Ψ_2, Ψ_3, Ψ_4, Φ_{22}, correspond to independent components of the Riemann tensor. We shall call these four NP scalars "NP-null scalars." Since Ψ_2, Φ_{22} are real and Ψ_3, Ψ_4 are complex in Eq. (15) by applying the null condition, the NP-null scalars have six real d.o.f. as shown in the table below:

NP scalars		NP-null scalars
Ψ_0, Ψ_1, Ψ_2, Ψ_3, Ψ_4 Φ_{02}, Φ_{12}, Φ_{01}, Φ_{00}, Φ_{11}, Φ_{22}, Φ_{10}, Φ_{21}, Φ_{20} Λ	$\xrightarrow{\text{null condition}}$	Ψ_2, Ψ_3, Ψ_4, Φ_{22}

These six real d.o.f. of the NP-null scalars correspond to the polarization amplitudes p_n via Eq. (6),

$$\begin{aligned}
&\Psi_2 \overset{\text{null}}{\rightarrow} \frac{1}{6}R_{lklk} = \frac{1}{6}R_{tztz} \equiv \frac{1}{6}p_1^{(l)}(\vec{k}, t),\\
&\mathrm{Re}(\Psi_3) \overset{\text{null}}{\rightarrow} \frac{1}{2}\mathrm{Re}(R_{lkl\bar{m}}) \overset{\text{null}}{\rightarrow} \frac{1}{2}R_{tztx} \equiv \frac{1}{2}p_2^{(x)}(\vec{k}, t),\\
&\mathrm{Im}(\Psi_3) \overset{\text{null}}{\rightarrow} \frac{1}{2}\mathrm{Im}(R_{lkl\bar{m}}) \overset{\text{null}}{\rightarrow} -\frac{1}{2}R_{tzty} \equiv -\frac{1}{2}p_3^{(y)}(\vec{k}, t),\\
&\mathrm{Re}(\Psi_4) \overset{\text{null}}{\rightarrow} \mathrm{Re}(R_{l\bar{m}l\bar{m}}) \overset{\text{null}}{\rightarrow} R_{txtx} - R_{tyty} \equiv p_4^{(+)}(\vec{k}, t),\\
&\mathrm{Im}(\Psi_4) \overset{\text{null}}{\rightarrow} \mathrm{Im}(R_{l\bar{m}l\bar{m}}) \overset{\text{null}}{\rightarrow} -2R_{txty} \equiv -2p_5^{(\times)}(\vec{k}, t),\\
&\Phi_{22} \overset{\text{null}}{\rightarrow} R_{lml\bar{m}} \overset{\text{null}}{\rightarrow} R_{txtx} + R_{tyty} \equiv p_6^{(b)}(\vec{k}, t),
\end{aligned} \tag{16}$$

and the driving-force matrix (5) is written under the null-propagation condition in terms of the NP-null scalars as

$$S_{\text{null}} = \begin{pmatrix} \frac{1}{2}[\mathrm{Re}(\Psi_4) + \Phi_{22})] & -\frac{1}{2}\mathrm{Im}(\Psi_4) & 2\mathrm{Re}(\Psi_3) \\ -\frac{1}{2}\mathrm{Im}(\Psi_4) & -\frac{1}{2}[\mathrm{Re}(\Psi_4) - \Phi_{22}] & -2\mathrm{Im}(\Psi_3) \\ 2\mathrm{Re}(\Psi_3) & -2\mathrm{Im}(\Psi_3) & 6\Psi_2 \end{pmatrix}. \tag{17}$$

The polarization amplitudes p_n in Eq. (16) are different from those in Ref. [1]. First, the overall sign in Eq. (16) is opposite to that in Ref. [1] since we used the definition of the NP scalars in Ref. [31]. Second, each p_n in Eq. (16) has a different coefficient since the basis polarization matrices in Eq. (3) chose different normalization coefficients. The six normalization coefficients a_n are introduced as

$$E_1(\hat{z}) = a_1\begin{pmatrix}0&0&0\\0&0&0\\0&0&1\end{pmatrix},\qquad E_2(\hat{z}) = a_2\begin{pmatrix}0&0&1\\0&0&0\\1&0&0\end{pmatrix},$$
$$E_3(\hat{z}) = a_3\begin{pmatrix}0&0&0\\0&0&1\\0&1&0\end{pmatrix},\qquad E_4(\hat{z}) = a_4\begin{pmatrix}1&0&0\\0&-1&0\\0&0&0\end{pmatrix},$$
$$E_5(\hat{z}) = a_5\begin{pmatrix}0&1&0\\1&0&0\\0&0&0\end{pmatrix},\qquad E_6(\hat{z}) = a_6\begin{pmatrix}1&0&0\\0&1&0\\0&0&0\end{pmatrix},\qquad (18)$$

and their values are given in the table below:

	a_1	a_2	a_3	a_4	a_5	a_6
(3)	1	1	1	$\frac{1}{2}$	1	$\frac{1}{2}$
Ref. [1]	-6	-2	2	$-\frac{1}{2}$	$\frac{1}{2}$	$-\frac{1}{2}$

Subsequently, the polarization amplitudes p_n in Eq. (16) are related to the corresponding amplitudes $\bar{p}_n$ in Ref. [1],

$$p_1^{(l)} = -6\bar{p}_1^{(l)},\quad p_2^{(x)} = -2\bar{p}_2^{(x)},\quad p_3^{(y)} = 2\bar{p}_3^{(y)},$$
$$p_4^{(+)} = -\bar{p}_4^{(+)},\quad p_5^{(\times)} = \frac{1}{2}\bar{p}_5^{(\times)},\quad p_6^{(b)} = -\bar{p}_6^{(b)}.\qquad (19)$$

The driving-force matrix $S_{\rm null}$ for the null condition in Eq. (17), which is a physical quantity, coincides exactly irrespective of the choice of the normalization constants in Eq. (18).

B. Non-null propagation of gravitational waves in terms of NP scalars

The gravitational waves generated by some gravitational theories may propagate along non-null geodesics. Since the NP formalism (16) obtained under the null condition (14) can no longer be applied to those, it is necessary to find the six polarization amplitudes $p_n (p = 1, 2, \ldots, 6)$ before assigning the null condition. The exact polarization amplitudes expressed in terms of the electric components of the Riemann tensor are easily obtained by inverting the five complex Weyl-NP scalars (10) and the ten Ricci-NP scalars (11),

$$p_1^{(l)} = R_{tztz} = 2[\mathrm{Re}(\Psi_2) + \Phi_{11} - \Lambda],$$
$$p_2^{(x)} = R_{tztx} = -\mathrm{Re}(\Psi_1) + \mathrm{Re}(\Psi_3) - \mathrm{Re}(\Phi_{01}) + \mathrm{Re}(\Phi_{12}),$$
$$p_3^{(y)} = R_{tzty} = -\mathrm{Im}(\Psi_1) - \mathrm{Im}(\Psi_3) - \mathrm{Im}(\Phi_{01}) + \mathrm{Im}(\Phi_{12}),$$
$$p_4^{(+)} = R_{txtx} - R_{tyty} = \mathrm{Re}(\Psi_0) + \mathrm{Re}(\Psi_4) - 2\mathrm{Re}(\Phi_{02}),$$
$$p_5^{(\times)} = R_{txty} = \frac{1}{2}[\mathrm{Im}(\Psi_0) - \mathrm{Im}(\Psi_4) - 2\mathrm{Im}(\Phi_{02})],$$
$$p_6^{(b)} = R_{txtx} + R_{tyty} = -2\mathrm{Re}(\Psi_2) + \Phi_{00} + \Phi_{22} - 4\Lambda.\qquad (20)$$

The exact NP expressions valid for plane-wave amplitudes of gravitational waves are obtained by assigning the condition of the plane-wave propagation along the z direction to the components of the Riemann tensor. Specifically, every component of the Riemann tensor for the plane wave is a function of time t and propagation coordinate z including the retarded time with v, $t_{\rm r} = t - z/v$, $R_{\mu\nu\rho\sigma} = R_{\mu\nu\rho\sigma}(t, z)$, which satisfies

$$R_{\mu\nu\rho\sigma,p} = 0,\qquad (21)$$

where v is the speed of the gravitational wave, and (μ, ν, ρ, σ) range over (t, x, y, z) and $(p, q, r, \cdots)$ only range over (x, y). Except for trivial non-wave-like constant solutions that are of no interest here, the Bianchi identity $R_{\mu\nu[pq,t]} = 0 = \frac{1}{3}R_{\mu\nu pq,t}$ supports some null curvature solutions for gravitational waves,

$$R_{\mu\nu pq} = 0.\qquad (22)$$

Since the Ricci and Einstein tensors are related to the polarization amplitudes as

$$p_1^{(l)} = \frac{1}{2}(G_{tt} + G_{xx} + G_{yy} - G_{zz}) - R_{xyxy} \overset{\text{plane}}{\underset{\text{wave}}{\rightarrow}} \frac{1}{2}(G_{tt} + G_{xx} + G_{yy} - G_{zz}),$$
$$p_2^{(x)} = -G_{xz} + R_{zyxy} \overset{\text{plane}}{\underset{\text{wave}}{\rightarrow}} -G_{xz},$$
$$p_3^{(y)} = -G_{yz} - R_{zxxy} \overset{\text{plane}}{\underset{\text{wave}}{\rightarrow}} -G_{yz},$$
$$p_4^{(+)} = -(G_{xx} - G_{yy}) + R_{zxzx} - R_{zyzy} \overset{\text{plane}}{\underset{\text{wave}}{\rightarrow}} -(G_{xx} - G_{yy}) + R_{zxzx} - R_{zyzy},$$
$$p_5^{(\times)} = -G_{xy} + R_{zxzy} \overset{\text{plane}}{\underset{\text{wave}}{\rightarrow}} -G_{xy} + R_{zxzy},$$
$$p_6^{(b)} = G_{zz} + R_{xyxy} \overset{\text{plane}}{\underset{\text{wave}}{\rightarrow}} G_{zz},\qquad (23)$$

the plane-wave condition (22) enables us to easily read vanishing nontensorial polarization modes in the Ricci-flat spacetime. This is consistent with the well-known fact that Einstein gravity only supports two tensorial modes for plane-wave gravitational waves on a flat background because of the Ricci-flat condition. The plane-wave condition (22) allows us to write these six conditions for the z propagation in terms of the NP scalars,

$$\Psi_1 = \Phi_{01}, \qquad \Psi_2 = \Phi_{11} + \Lambda, \qquad \Psi_3 = \Phi_{21}. \tag{24}$$

Since Φ_{11} and Λ are real, the second condition implies that Ψ_2 is real. Substituting these relations into the polarization amplitudes in Eq. (20) expresses them in terms of the nine NP scalars, $\Psi_0, \Psi_1, \Psi_2, \Psi_3, \Psi_4, \Phi_{00}, \Phi_{02}, \Phi_{22}, \Lambda$. Since $\Psi_0, \Psi_1, \Psi_3, \Psi_4, \Phi_{02}$ are complex, the nine NP scalars represent the fourteen components of the Riemann curvature tensor, which says that the NP scalars are inconvenient to describe the polarization amplitudes p_n for the non-null geodesic. In each p_n, there are two contributions: the term which survives under the null condition and the terms in the square brackets, which vanish for null propagation,

$$\begin{aligned}
p_1^{(l)} &= 6\Psi_2 - [2(\Psi_2 + 2\Lambda)],\\
p_2^{(x)} &= 2\mathrm{Re}(\Psi_3) - [2\mathrm{Re}(\Psi_1)],\\
p_3^{(y)} &= -2\mathrm{Im}(\Psi_3) - [2\mathrm{Im}(\Psi_1)],\\
p_4^{(+)} &= \mathrm{Re}(\Psi_4) + [\mathrm{Re}(\Psi_0) - 2\mathrm{Re}(\Phi_{02})],\\
p_5^{(\times)} &= -\frac{1}{2}\mathrm{Im}(\Psi_4) + \left[\frac{1}{2}\mathrm{Im}(\Psi_0) - \mathrm{Im}(\Phi_{02})\right],\\
p_6^{(b)} &= \Phi_{22} - [2(\Psi_2 + 2\Lambda) - \Phi_{00}].
\end{aligned} \tag{25}$$

It is easily checked that the null condition in Eq. (15) makes the deviation factors in the square brackets vanish. In the scalar longitudinal ($p_1^{(l)}$) and breathing ($p_6^{(b)}$) modes, the common factor $\Psi_2 + 2\Lambda$ contributes to the deviation and $p_6^{(b)}$ has an additional deviation from the NP scalar Φ_{00} of spin weight 0. The Weyl-NP scalars Ψ_1 and Ψ_3 of spin weight ± 1 are mixed in the vector-x ($p_2^{(x)}$) and -y ($p_3^{(y)}$) modes. The tensor component Ψ_4 is also mixed with the other scalars of spin weight ± 2 [Ψ_0, Φ_{02}, and $\Phi_{20}(=\Phi_{02}^*)$] in the plus ($p_4^{(+)}$) and cross ($p_5^{(\times)}$) polarization modes. Consequently, the driving-force matrix (5) for plane-wave propagation becomes

$$S_{\mathrm{plane}} = \begin{pmatrix}
\frac{1}{2}\{\mathrm{Re}(\Psi_4) + \Phi_{22} + [\mathrm{Re}(\Psi_0) - 2\mathrm{Re}(\Phi_{02}) \\ \quad -2(\Psi_2 + 2\Lambda) + \Phi_{00}]\} & -\frac{1}{2}\{\mathrm{Im}(\Psi_4) \\ \quad -[\mathrm{Im}(\Psi_0) - 2\mathrm{Im}(\Phi_{02})]\} & 2\{\mathrm{Re}(\Psi_3) \\ \quad -[\mathrm{Re}(\Psi_1)]\} \\
-\frac{1}{2}\{\mathrm{Im}(\Psi_4) \\ \quad -[\mathrm{Im}(\Psi_0) - 2\mathrm{Im}(\Phi_{02})]\} & -\frac{1}{2}\{\mathrm{Re}(\Psi_4) - \Phi_{22} \\ \quad +[\mathrm{Re}(\Psi_0) - 2\mathrm{Re}(\Phi_{02}) \\ \quad +2(\Psi_2 + 2\Lambda) - \Phi_{00}]\} & -2\{\mathrm{Im}(\Psi_3) \\ \quad +[\mathrm{Im}(\Psi_1)]\} \\
2\{\mathrm{Re}(\Psi_3) - [\mathrm{Re}(\Psi_1)]\} & -2\{\mathrm{Im}(\Psi_3) + [\mathrm{Im}(\Psi_1)]\} & 6\{\Psi_2 - [\frac{1}{3}(\Psi_2 + 2\Lambda)]\}
\end{pmatrix} \tag{26}$$

Note that the terms in the square brackets in Eq. (25) are generally nonvanishing, which means that there are two sources of deviation factors for non-null propagation of gravitational waves: the NP-null scalars in the first terms of Eq. (25), and the other NP scalars in the square brackets of Eq. (25). Therefore, the computation and analysis of the polarization amplitudes for the non-null geodesic using the NP-null scalars (16) [10,17–20] are incorrect as long as the terms in the square brackets are nonvanishing. Thus, the correction factors of deviation in the square brackets of Eq. (25) and/or Eq. (26) should be taken into account in order to achieve the correct exact polarization amplitude for the non-null propagation of gravitational waves. Furthermore, for the non-null propagation of gravitational waves, Ψ_2 is mixed in the breathing mode $p_6^{(b)}$ in the last line of Eq. (25), which implies that a vanishing Φ_{22} does not imply a vanishing breathing mode, $p_6^{(b)} = -2\Psi_2$, even when $\Lambda = 0 = \Phi_{00}$.

C. Non-null propagation of gravitational waves in terms of metric perturbations

In this subsection, we read the exact polarization amplitudes p_n from the driving-force matrix without relying on NP scalars. By taking into account the weak field assumption, the Riemann tensor is linearized as

$$R^{(1)}_{\mu\nu\rho\sigma} = -2\partial_{[\mu}\partial_{|[\rho}h_{\sigma]|\nu]}, \tag{27}$$

where the superscript $^{(1)}$ denotes the order in h. Then, the polarization amplitudes p_n are described in terms of the metric perturbation,

$$\begin{aligned}
p_1^{(l)} &\approx R^{(1)}_{tztz} = -\frac{1}{2}(\partial_t^2 h_{zz} - 2\partial_t\partial_z h_{tz} + \partial_z^2 h_{tt}),\\
p_2^{(x)} &\approx R^{(1)}_{tztx} = -\frac{1}{2}(\partial_t^2 h_{xz} - \partial_t\partial_z h_{tx}),
\end{aligned}$$

$$p_3^{(y)} \approx R^{(1)}_{tzty} = -\frac{1}{2}(\partial_t^2 h_{yz} - \partial_t\partial_z h_{ty}),$$
$$p_4^{(+)} \approx R^{(1)}_{txtx} - R^{(1)}_{tyty} = -\frac{1}{2}(\partial_t^2 h_{xx} - \partial_t^2 h_{yy}),$$
$$p_5^{(\times)} \approx R^{(1)}_{txty} = -\frac{1}{2}\partial_t^2 h_{xy},$$
$$p_6^{(b)} \approx R^{(1)}_{txtx} + R^{(1)}_{tyty} = -\frac{1}{2}(\partial_t^2 h_{xx} + \partial_t^2 h_{yy}). \quad (28)$$

Since all ten components of the metric perturbation $h_{\mu\nu}$ appear on the right-hand sides of Eq. (28), four redundant d.o.f. should be removed by the gauge fixing. In the following two subsubsections, we discuss the Lorentz and Newtonian gauge conditions.

1. Lorentz gauge condition

The production and propagation of gravitational waves from various massive dynamical systems are calculated under the Lorentz gauge condition $\partial_\mu \bar{h}^{\mu\nu} \equiv \partial_\mu(h^{\mu\nu} - \frac{1}{2}\eta^{\mu\nu}h^\lambda_\lambda) = 0$ in Einstein gravity. This gauge is also often used to describe wave-like solutions. The four components of the Lorentz gauge condition are

$$\partial_t h_{tz} - \partial_z h_{xz} = 0,$$
$$\partial_t h_{ty} - \partial_z h_{yz} = 0,$$
$$(\partial_t^2 - \partial_z^2)h_{tz} = -\partial_t\partial_z(h_{xx} + h_{yy}),$$
$$(\partial_t^2 - \partial_z^2)(h_{tt} + h_{zz}) = -(\partial_t^2 + \partial_z^2)(h_{xx} + h_{yy}). \quad (29)$$

By removing the four time components h_{tt}, h_{tx}, h_{ty}, h_{tz} by applying the gauge-fixing condition in Eq. (29), we obtain a set of nonlocal expressions for the polarization amplitudes,

$$p_1^{(l)} = -\frac{1}{2}[\partial_z^2(h_{xx} + h_{yy}) + (\partial_t^2 - \partial_z^2)h_{zz}],$$
$$p_2^{(x)} = -\frac{1}{2}(\partial_t^2 - \partial_z^2)h_{xz},$$
$$p_3^{(y)} = -\frac{1}{2}(\partial_t^2 - \partial_z^2)h_{yz},$$
$$p_4^{(+)} = -\frac{1}{2}\partial_t^2(h_{xx} - h_{yy}),$$
$$p_5^{(\times)} = -\frac{1}{2}\partial_t^2 h_{xy},$$
$$p_6^{(b)} = -\frac{1}{2}\partial_t^2(h_{xx} + h_{yy}). \quad (30)$$

So far, all of the expressions in Eq. (30) are still linear in the metric perturbation, and the would-be dynamical equation for $h_{\mu\nu}$ approximated in the weak-gravity limit is naturally expected to be a linear wave equation which supports the monochromatic wave solution of the form

$$h_{\mu\nu} = C_{\mu\nu}e^{-i\omega t + ikz}, \quad (31)$$

where ω is the frequency and k is the wave number. The linearity of the assumed wave equation guarantees that the spacetime-independent coefficients C_{ij} are also independent of the frequency ω and wave number k. Substituting the monochromatic wave solution (31) into the gauge-fixing condition (30) leads to

$$h_{tx} = -\frac{k}{\omega}h_{xz}, \qquad h_{ty} = -\frac{k}{\omega}h_{yz},$$
$$h_{tz} = \frac{\omega k}{\omega^2 - k^2}(h_{xx} + h_{yy}),$$
$$h_{tt} = -h_{zz} - \frac{\omega^2 + k^2}{\omega^2 - k^2}(h_{xx} + h_{yy}), \quad (32)$$

which tells us that the other four coefficients C_{tt}, C_{tx}, C_{ty}, C_{tz} depend on the frequency ω and the wave number k. Then the six polarization amplitudes p_n are expressed in terms of the six spatial components of the metric fluctuation:

$$p_1^{(l)} = \frac{1}{2}[k^2(h_{xx} + h_{yy}) + (\omega^2 - k^2)h_{zz}],$$
$$p_2^{(x)} = \frac{1}{2}(\omega^2 - k^2)h_{xz},$$
$$p_3^{(y)} = \frac{1}{2}(\omega^2 - k^2)h_{yz},$$
$$p_4^{(+)} = \frac{1}{2}\omega^2(h_{xx} - h_{yy}),$$
$$p_5^{(\times)} = \frac{1}{2}\omega^2 h_{xy},$$
$$p_6^{(b)} = \frac{1}{2}\omega^2(h_{xx} + h_{yy}). \quad (33)$$

If the limit of Einstein gravity is naively taken, the dispersion relation becomes $\omega^2 = k^2$ and the four modes $p_1^{(l)}, p_4^{(+)}, p_5^{(\times)}, p_6^{(b)}$ seem to be nonvanishing in Eq. (33), which is inconsistent with the fact that only the two tensor modes $p_4^{(+)}$ and $p_5^{(\times)}$ should survive. To correctly reproduce these physical modes, the transverse-traceless condition, $\partial_\mu h^\mu_\nu = 0$ and $h^\mu_\mu = 0$, should also be imposed.

It would be convenient to avoid this cumbersome additional condition and obtain the two tensor modes in the limit of Einstein gravity. A specific way is to remove h_{xx} from the physical components and to include h_{tt} as a physical mode. The corresponding monochromatic wave solution (31) allows for a new assumption on $C_{\mu\nu}$, i.e., that

$$C_{tt}, C_{yy}, C_{zz}, C_{xy}, C_{yz}, C_{zx} \quad (34)$$

are independent of the frequency ω and the wave number k. On the other hand, the four gauge conditions in Eq. (32) force the remaining four $(C_{xx}, C_{tx}, C_{ty}, C_{tz})$ to be functions of ω and k,

$$h_{tx} = -\frac{k}{\omega} h_{xz}, \qquad h_{ty} = -\frac{k}{\omega} h_{yz},$$
$$h_{tz} = -\frac{\omega k}{\omega^2 + k^2}(h_{tt} + h_{zz}),$$
$$h_{xx} = -h_{yy} - \frac{\omega^2 - k^2}{\omega^2 + k^2}(h_{tt} + h_{zz}). \tag{35}$$

Thus, the gauge-fixing condition (32) reexpresses the polarization amplitudes p_n as

$$p_1^{(l)} = \frac{1}{2}\left(\frac{\omega^2 - k^2}{\omega^2 + k^2}\right)\omega^2(h_{tt} + h_{zz}) - \frac{1}{2}(\omega^2 - k^2)h_{tt},$$
$$p_2^{(x)} = \frac{1}{2}(\omega^2 - k^2)h_{xz},$$
$$p_3^{(y)} = \frac{1}{2}(\omega^2 - k^2)h_{yz},$$
$$p_4^{(+)} = -\frac{1}{2}\left(\frac{\omega^2 - k^2}{\omega^2 + k^2}\right)\omega^2(h_{tt} + h_{zz}) - \omega^2 h_{yy},$$
$$p_5^{(\times)} = \frac{1}{2}\omega^2 h_{xy},$$
$$p_6^{(b)} = -\frac{1}{2}\left(\frac{\omega^2 - k^2}{\omega^2 + k^2}\right)\omega^2(h_{tt} + h_{zz}). \tag{36}$$

The deviation from the null geodesic appears through the separate term in every mode controlled by the nonvanishing common factor $\omega^2 - k^2$ in the five polarization amplitudes $p_1^{(l)}$, $p_2^{(x)}$, $p_3^{(y)}$, $p_4^{(+)}$, and $p_6^{(b)}$. Thus, the survival of only the two tensor modes in the limit of the null geodesic is automatically reproduced without any further condition by applying the dispersion relation $\omega = k$ which makes the common factor vanish, $\omega^2 - k^2 = 0$. The magnitude of this additional effect is quantitatively determined by the specific form of the dispersion relation, $\omega = \omega(k)$. Accordingly, the NP-null scalars under the same gauge-fixing condition (32) are

$$\Psi_2 = -\frac{1}{24}\left(\frac{\omega^2 - k^2}{\omega^2 + k^2}\right)[(3k^2 - \omega^2)h_{tt} + (k^2 - 3\omega^2)h_{zz}],$$
$$\Psi_3 = \frac{1}{8}\frac{(\omega - k)(\omega + k)^2}{\omega}(h_{xz} - ih_{yz}),$$
$$\Psi_4 = -\frac{1}{8}\frac{(\omega - k)(\omega + k)^3}{\omega^2 + k^2}(h_{tt} + h_{zz}) - \frac{1}{4}(\omega + k)^2(h_{yy} + ih_{xy}),$$
$$\Phi_{22} = -\frac{1}{8}\frac{(\omega - k)(\omega + k)^3}{\omega^2 + k^2}(h_{tt} + h_{zz}). \tag{37}$$

2. Newtonian gauge condition

When the general metric perturbations are decomposed in the basis of the representations of the spatial rotation, all 16 components are

$$\delta g_{00} = -2A,$$
$$\delta g_{0i} = -\partial_i B - B_i,$$
$$\delta g_{ij} = -2\delta_{ij}D + 2\left(\partial_i\partial_j - \frac{\delta_{ij}}{3}\partial^k\partial_k\right)E + 2\partial_{(i}E_{j)} + h_{ij}, \tag{38}$$

where the symmetric property is recovered by the following six rotations: $\partial^i B_i = 0$, $\partial^i E_i = 0$, $\partial^i h_{ij} = 0$, and $h^i_i = 0$. Then, the ten modes are decoupled at the linear level of this decomposition. In the representation of the spatial rotation about the specific $\hat{z}$ axis, the metric perturbation $h_{\mu\nu}$ takes the following matrix form:

$$h_{\mu\nu} = \begin{pmatrix} -2A & -B_x & -B_y & -B_{,z} \\ -B_x & -2D - \frac{2}{3}E_{,zz} + h_+ & h_\times & E_{x,z} \\ -B_y & h_\times & -2D - \frac{2}{3}E_{,zz} - h_+ & E_{y,z} \\ -B_{,z} & E_{x,z} & E_{y,z} & -2D + \frac{4}{3}E_{,zz} \end{pmatrix}. \tag{39}$$

Inserting this into the six polarization amplitudes p_n [Eq. (28)] leads to

$$p_1^{(l)} = \partial_t^2 D - \frac{2}{3}\partial_t^2(E_{,zz}) - \partial_t\partial_z(B_{,z}) + \partial_z^2 A,$$
$$p_2^{(x)} = -\frac{1}{2}[\partial_t^2(E_{x,z}) + \partial_t\partial_z B_x],$$
$$p_3^{(y)} = -\frac{1}{2}[\partial_t^2(E_{y,z}) + \partial_t\partial_z B_y],$$
$$p_4^{(+)} = -\partial_t^2 h_+,$$
$$p_5^{(\times)} = -\frac{1}{2}\partial_t^2 h_\times,$$
$$p_6^{(b)} = 2\partial_t^2 D + \frac{2}{3}\partial_t^2(E_{,zz}). \tag{40}$$

An appropriate gauge-fixing condition for this decomposition is the conformal Newtonian gauge, $B_x = B_y = B = E = 0$, which results in $h_{tx} = h_{ty} = h_{tz} = 0$ and $h_{xx} + h_{yy} = 2h_{zz}$. Under this gauge-fixing condition, the above six polarization amplitudes p_n become

$$\begin{aligned} p_1^{(l)} &= \partial_t^2 D + \partial_z^2 A, \\ p_2^{(x)} &= -\frac{1}{2}\partial_t^2 (E_{x,z}), \\ p_3^{(y)} &= -\frac{1}{2}\partial_t^2 (E_{y,z}), \\ p_4^{(+)} &= -\partial_t^2 h_+, \\ p_5^{(\times)} &= -\frac{1}{2}\partial_t^2 h_\times, \\ p_6^{(b)} &= 2\partial_t^2 D. \end{aligned} \tag{41}$$

For the monochromatic waves, Eq. (41) gives

$$\begin{aligned} p_1^{(l)} &= -\omega^2 D - k^2 A, \\ p_2^{(x)} &= \frac{1}{2}\omega^2 (E_{x,z}), \\ p_3^{(y)} &= \frac{1}{2}\omega^2 (E_{y,z}), \\ p_4^{(+)} &= \omega^2 h_+, \\ p_5^{(\times)} &= \frac{1}{2}\omega^2 h_\times, \\ p_6^{(b)} &= -2\omega^2 D. \end{aligned} \tag{42}$$

D. Response function

In gravitational-wave detectors, the phase difference between the light signals traveling in both arms of the interferometer is given by

$$\Delta\Phi = 2\pi\nu(2L_1 - 2L_2) \equiv 2\pi\nu L_0 S(t), \tag{43}$$

where ν is the frequency of the laser light, L_0 is the length of the unperturbed interferometer arm, L_1 and L_2 are the perturbed lengths of the two arms, and $S(t)$ is the detector's response function [4,32]. The response function $S(t)$ is written in terms of the theoretically obtained polarization amplitudes p_n multiplied by the normalization coefficients a_n of the basis polarization matrices in Eq. (3) and the angular pattern function F_n,

$$S(t) = \sum_{n=1}^{6} 2\tilde{p}_n a_n F_n, \tag{44}$$

where $p_n \equiv -\ddot{\tilde{p}}_n$. The angular pattern functions F_n have five different components as in Refs. [4,32],

$$F_b = -\frac{1}{2}\sin^2\theta\cos 2\phi = -F_l, \tag{45}$$

$$F_x = -\sin\theta(\cos\theta\cos 2\phi\cos\psi - \sin 2\phi\sin\psi), \tag{46}$$

$$F_y = -\sin\theta(\cos\theta\cos 2\phi\sin\psi + \sin 2\phi\cos\psi), \tag{47}$$

$$F_+ = \frac{1}{2}(1+\cos^2\theta)\cos 2\phi\cos 2\psi - \cos\theta\sin 2\phi\sin 2\psi, \tag{48}$$

$$F_\times = \frac{1}{2}(1+\cos^2\theta)\cos 2\phi\sin 2\psi - \cos\theta\sin 2\phi\cos 2\psi. \tag{49}$$

As long as the gravitational wave along the light trajectory is weak, the response function is generally given by a superposition of the contributions of monochromatic gravitational waves. For each monochromatic wave of frequency ω, it satisfies $\tilde{p}_n = \frac{1}{\omega^2} p_n$, and thus the response function (44) becomes

$$S(t) \equiv \sum_{n=1}^{6} S_n(t) = \sum_{n=1}^{6} 2\frac{p_n}{\omega^2} a_n F_n. \tag{50}$$

Note that the value of each $p_n a_n$ is independent of the choice of the basis matrix (18) and each response function S_n,

$$S_n = 2\tilde{p}_n a_n F_n = -\frac{2}{\partial_t^2} p_n a_n F_n, \tag{51}$$

is gauge invariant. We read six response functions in terms of the metric components in the nonlocal expression,

$$\begin{aligned} S^{(l)} &= \frac{1}{\partial_t^2}(\partial_t^2 h_{zz} - 2\partial_t\partial_z h_{tz} + \partial_z^2 h_{tt})F_l, \\ S^{(x)} &= \frac{1}{\partial_t^2}(\partial_t^2 h_{xz} - \partial_t\partial_z h_{tx})F_x, \\ S^{(y)} &= \frac{1}{\partial_t^2}(\partial_t^2 h_{yz} - \partial_t\partial_z h_{ty})F_y, \\ S^{(+)} &= \frac{1}{2\partial_t^2}\partial_t^2(h_{xx} - h_{yy})F_+, \\ S^{(\times)} &= \frac{1}{\partial_t^2}\partial_t^2 h_{xy} F_\times, \\ S^{(b)} &= \frac{1}{2\partial_t^2}\partial_t^2(h_{xx} + h_{yy})F_b. \end{aligned} \tag{52}$$

As in Eq. (45), the angular pattern functions of the longitudinal mode and the breathing mode are the same, $F_b = -F_l$, and the breathing and longitudinal pattern functions are degenerated. Thus, no array of laser interferometers can measure their two modes separately [4]. In addition to the four pattern functions $S^{(x)}, S^{(y)}, S^{(+)}, S^{(\times)}$, the single response function given by the sum of the longitudinal and breathing modes,

$$S^{(l+b)} = \frac{1}{\partial_t^2}\left\{\partial_t^2\left[h_{zz} - \frac{1}{2}(h_{xx}+h_{yy})\right] - 2\partial_t\partial_z h_{tz} + \partial_z^2 h_{tt}\right\}F_l, \tag{53}$$

is taken into account. When a monochromatic wave [Eq. (31)] is assumed, the five response functions become

$$\begin{aligned} S^{(x)} &= \left(h_{xz} + \frac{k}{\omega}h_{tx}\right)F_x, \\ S^{(y)} &= \left(h_{yz} + \frac{k}{\omega}h_{ty}\right)F_y, \\ S^{(+)} &= \frac{1}{2}(h_{xx}-h_{yy})F_+, \\ S^{(\times)} &= h_{xy}F_\times, \end{aligned}$$

and

$$S^{(l+b)} = \left\{\left[h_{zz} - \frac{1}{2}(h_{xx}+h_{yy})\right] + 2\frac{k}{\omega}h_{tz} + \frac{k^2}{\omega^2}h_{tt}\right\}F_l. \tag{54}$$

1. Lorentz gauge condition

When the Lorentz gauge condition (29) is chosen, the polarization amplitudes p_n were already obtained for a monochromatic wave in Eq. (33) and thus the five components of the response function are obtained. From Eq. (54), the response function for the breathing and longitudinal modes becomes

$$S^{(b+l)} = \left\{\frac{(\omega^2-k^2)}{\omega^2}[h_{zz} - (h_{xx}+h_{yy})] + \frac{1}{2}(h_{xx}+h_{yy})\right\}F_l,$$

and those for the other four modes are

$$\begin{aligned} S^{(x)} &= \frac{\omega^2-k^2}{\omega^2}h_{xz}F_x, \\ S^{(y)} &= \frac{\omega^2-k^2}{\omega^2}h_{yz}F_y, \\ S^{(+)} &= \frac{1}{2}(h_{xx}-h_{yy})F_+, \\ S^{(\times)} &= h_{xy}F_\times. \end{aligned} \tag{55}$$

As we already discussed, the response function for the breathing and longitudinal modes (57) does not vanish even in the null limit of $\omega^2 = k^2$ under the consideration of constant h_{ij}. Thus, in the Lorentz gauge, a convenient choice is to set C_{tt} constant as in Eq. (35) instead of C_{xx}. Note again that the six amplitudes of the gravitational wave C_{tt}, C_{yy}, C_{zz}, C_{xy}, C_{yz}, and C_{yx} do not depend on the frequency ω and the wave number k, which makes the detection of the polarization tractable. By using Eq. (36), the response function for the breathing and longitudinal modes becomes

$$S^{(b+l)} = \frac{(\omega^2-k^2)}{2\omega^2(\omega^2+k^2)}[(\omega^2-2k^2)h_{tt} + 3\omega^2 h_{zz}]F_l,$$

and those for the other four modes are

$$\begin{aligned} S^{(x)} &= \frac{\omega^2-k^2}{\omega^2}h_{xz}F_x, \\ S^{(y)} &= \frac{\omega^2-k^2}{\omega^2}h_{yz}F_y, \\ S^{(+)} &= \left[-h_{yy} - \frac{1}{2}\frac{\omega^2-k^2}{\omega^2+k^2}(h_{tt}+h_{zz})\right]F_+, \\ S^{(\times)} &= h_{xy}F_\times. \end{aligned} \tag{56}$$

As expected, there is an overall $(\omega^2 - k^2)$ factor in $S^{(b+l)}$, $S^{(x)}$, and $S^{(y)}$, which allows them to vanish continuously in the null limit.

2. Newtonian gauge condition

Similar to the Lorentz gauge condition, the response function for the breathing and longitudinal modes is given under the Newtonian gauge condition (38) as

$$S^{(b+l)} = \frac{k^2}{\omega^2}h_{tt}F_l, \tag{57}$$

and those of the other four amplitudes are

$$\begin{aligned} S^{(x)} &= h_{xz}F_x, \\ S^{(y)} &= h_{yz}F_y, \\ S^{(+)} &= h_+F_+, \\ S^{(\times)} &= h_{xy}F_\times. \end{aligned} \tag{58}$$

Since all five amplitudes of the monochromatic gravitational wave are constants, the four response functions $S^{(x)}, S^{(y)}, S^{(+)}$, and $S^{(\times)}$ involve no dependence on the frequency ω and wave number k; however, $S^{(b+l)}$ does depend on the frequency and wave number.

IV. MODEL CALCULATION

The discussion up to Sec. III has been made without assuming a specific form of the wave equation; equivalently, the form of the action for gravity (and thus the

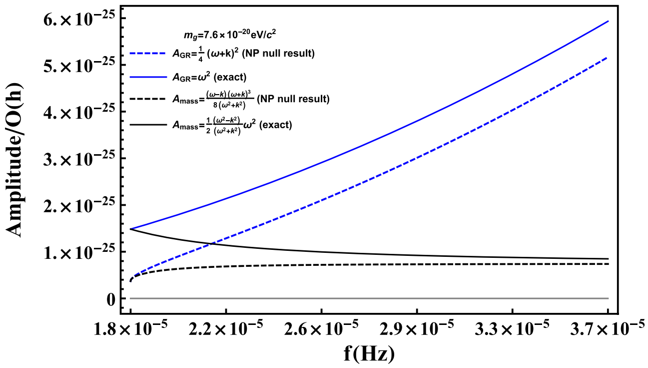

FIG. 2. The behavior of the exact (solid lines) and approximate (dashed lines) polarization amplitudes are compared by choosing a mass parameter $m_{\rm g} = 7.6 \times 10^{-20}$ eV/c^2 of the dispersion relation $\omega = \sqrt{m_{\rm g}^2 + k^2}$. The mode amplitude appearing for the time-like geodesic and that for the null geodesic are also compared by the black and blue curves.

polarization amplitudes p_n [Eq. (33)]) can be applicable to any null or non-null propagation of gravitational waves from arbitrary metric-compatible gravity theories. In this section, we consider an alternative model of gravity as an example and examine the polarization modes of the massive graviton. General dispersion relations shown in the literature will be discussed in the Appendix.

To investigate the behavior of the six polarization amplitudes, we already constructed the formalism and thus only need to specify the dispersion relation $\omega = \omega(k)$ according to the model of interest. Even when the wave equation does not involve higher-derivative terms, the relativistic relation between energy and momentum does not prohibit the mass term,

$$E^2 = p^2 + m_{\rm g}^2, \tag{59}$$

whose dispersion relation is $\omega = \pm\sqrt{m_{\rm g}^2 + k^2}$. Since the general covariance protects the introduction of a mass term in metric-compatible gravity theories and the Pauli-Fierz-type mass term for a spin-2 field is ruled out, a possible way to introduce the mass term with $g_{\mu\nu}$ is to employ the bimetric theory in which both the background metric $g^0_{\mu\nu}$ and the metric for the gravitational field $(g - g_0)_{\mu\nu}$ are tensor quantities [33].

The dispersion relation $\omega = \sqrt{m_{\rm g}^2 + k^2}$ can be used in the weak-gravity limit as far as the bimetric theory is considered. In $p_4^{(+)}$ [Eq. (36)], the second term $-\omega^2 h_{yy}$ is the plus-mode amplitude for the null geodesic and the first term $-\frac{1}{2}(\frac{\omega^2-k^2}{\omega^2+k^2})\omega^2(h_{tt} + h_{zz})$ appears for the time-like geodesic, which also coincides with the breathing mode amplitude $p_6^{(b)}$. These two exact amplitudes in $p_4^{(+)}$ [Eq. (6)] are compared to the corresponding approximate amplitudes of $\mathrm{Re}(\Psi_4)$ [Eq. (37)], and the result is given in Fig. 2. The blue and black solid lines denote ω^2 and $\frac{1}{2}\frac{\omega^2-k^2}{\omega^2+k^2}\omega^2$ in the exact amplitude, and the blue and black dashed lines denote $\frac{1}{4}(\omega + k)^2$ and $\frac{1}{8}\frac{(\omega-k)(\omega+k)^3}{\omega^2+k^2}$ in the approximate result. The graphs show that the behavior of the exact polarization amplitudes is different from that of the approximate polarization amplitudes obtained using NP-null scalars.

A comparison of the two solid lines in Fig. 2 shows the following. As easily expected, the effect due to the time-like geodesic becomes negligible in the high-frequency region. In the low-frequency region, the mode amplitude appearing for the time-like geodesic is magnified and becomes comparable to the mode amplitude for the null geodesic. The analogous conclusion was pointed out in the context of the approximate amplitudes obtained with the NP-null scalars [20], shown by the dashed lines in Fig. 2. The weakest bound of the graviton mass $m_{\rm g} = 7.6 \times 10^{-20}$eV/c^2 is chosen in Fig. 2 from the various model-independent mass bounds of the graviton, which are listed in Table I. The mode amplitude appearing for the time-like geodesic is significantly enhanced in the frequency region around 2×10^{-5} Hz. The frequency regions

TABLE I. The lower bounds of the Compton wavelength of the massive graviton $\lambda_{\rm g}$ and its corresponding upper bounds for the graviton mass $m_{\rm g} = h/\lambda_{\rm g}c$ from different observations. MD and MID mean model-dependent and model-independent, respectively. For details on the bounds, see Refs. [36,37].

$\lambda_{\rm g}$ (km)	$m_{\rm g}$ (eV/c^2)	Observation	Properties	References
2.8×10^{12}	4.4×10^{-22}	Solar system	Static, MID	[38,39]
1.7×10^{14}	8.0×10^{-24}	Solar system	Static, MID	[40]
2.5×10^{13}	5.0×10^{-23}	Supermassive black hole	Static, MID	[41]
6.2×10^{19}	2.0×10^{-29}	Galactic clusters	Static, MD	[42]
9.1×10^{19}	1.37×10^{-29}	Galaxy cluster Abell 1689	Static, MD	[43]
1.8×10^{22}	6.9×10^{-29}	Weak lensing	Static, MD	[44]
1.63×10^{10}	7.6×10^{-20}	Binary pulsars	Dynamical, MID	[45]
1.0×10^{13}	1.2×10^{-22}	Binary black holes	Dynamical, MID	[46]

TABLE II. The frequency regions where the massive effect on the polarization amplitudes becomes comparable to the massless one.

m_g (eV/c^2)	Observation	Frequency of massive effects (Hz)
4.4×10^{-22}	Solar system	1.06×10^{-7}
5.0×10^{-23}	Supermassive black holes	1.21×10^{-8}
2.0×10^{-29}	Galactic clusters	4.84×10^{-15}
6.9×10^{-29}	Weak lensing	1.67×10^{-14}
7.6×10^{-20}	Binary pulsars	1.84×10^{-5}
1.2×10^{-22}	Binary black holes	2.90×10^{-8}

of maximum enhancement are summarized in Table II, which overlap with the frequency domain of future detectors, such as the pulsar timing arrays with ranges of 10^{-9}–10^{-7} Hz [34,35]. As far as the amplitudes for the model-dependent mass bounds of the graviton are concerned, the maximum enhancement region occurs at ultralow frequencies, which have been dealt with in various inflation models but are too low to be detected by future planned detectors. As the detection level is increased with more accurate values, the suggested enhanced effect of the polarization modes due to the time-like geodesic may have a greater chance of being detected. In the very low-frequency region with the maximum enhancement, the deviation of the approximate result from the exact result also increases significantly, which is shown clearly in Fig. 3. Therefore, the exact formalism based on the time-like geodesic will play an important role in comparing the theoretical results with future observed data.

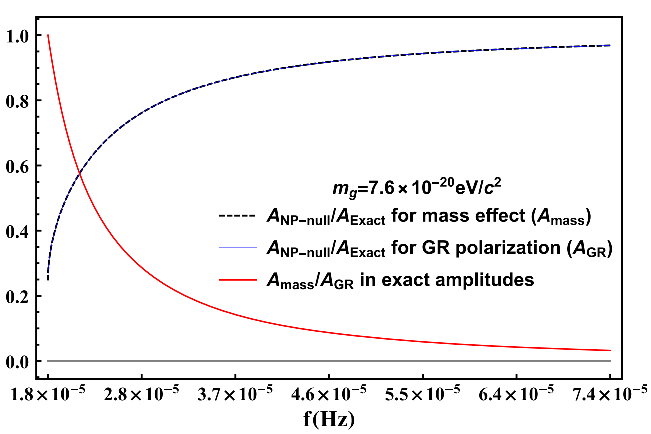

FIG. 3. The ratio between the approximate and exact mode amplitudes in the low-frequency region is shown for the weakest model-independent graviton mass bound. The more that the mode amplitude appearing for the time-like geodesic is enhanced, the greater the deviation of the approximate amplitude from the exact one grows.

V. CONCLUSION

We first extended the NP formalism to describe not only the null geodesic but also the time-like geodesic, which is necessary for massive gravity theories. The exact amplitudes of the six polarization modes were obtained in terms of the metric perturbation via the driving-force matrix (26) under a few gauge-fixing conditions: Eqs. (30) and (33) for the Lorentz gauge, Eq. (36) for our gauge choice, and Eqs. (41) and (42) for the Newtonian gauge. For a given frequency, the five corresponding distinctive response functions were constructed in Eqs. (56), (57), and (58), respectively. The formulas throughout this work are applicable to all metric-compatible gravity theories. Various theories have already been examined by using the formalism valid for the null geodesic, which is a good approximation for $\omega \gg m_g$. In the case of theories that include the non-null geodesic, it is definitely intriguing to reexamine the exact amplitudes of the six polarization modes, particularly for $\omega \gtrsim m_g$. As gravitational-wave detectors begin searching for signals coming from a theory beyond Einstein's GR, our construction of the general formalism will become more important.

Our final comment is about the classification of extended gravity theories. In Ref. [1], the null condition was used to classify the extended gravity theories [the E(2) classification] by using the little group of the polarization NP-null scalars. As explained in Ref. [1], the little group of the general Lorentz transformation for massless particles is given by the two-dimensional Euclidean group. In the case of time-like propagation, the little group of the Lorentz transformations corresponds to O(3), and therefore the classification should be made by considering this little group with the exact polarization expressions.

ACKNOWLEDGMENTS

Y.-H. H., Y. K., and S. L. are supported by the Basic Science Research Program through the National Research Foundation of Korea (NRF) funded by the Ministry of Science, ICT and Future Planning (Grants No. NRF-2018R1D1A1B07049514, NRF-2016R1D1A1B03931090, and NRF-2017R1A2B4011168, respectively). Y.-H. H. is also supported by the Korea Institute of Science and Technology Information (K-19-L02-C07-S01). We thank the anonymous referee for helpful comments.

APPENDIX: GENERALIZED DISPERSION RELATION

In this Appendix, we consider modified gravity theories with a generalized dispersion relation and show how the degenerate scalar response function described in terms of exact polarization amplitudes is used to read model parameters. As discussed in Refs. [47,48], the generalized dispersion relation that covers almost all theories of interest is

$$E^2 = p^2c^2 + m_g^2c^4 + Ap^\alpha c^\alpha, \tag{A1}$$

where the two parameters A and α express the violation of Lorentz symmetry. The speed of the graviton satisfying $E = \hbar\omega$ and $p = \hbar k$ is

$$\frac{v_g^2}{c^2} \equiv \frac{1}{c^2}\left(\frac{d\omega}{dk}\right)^2 = 1 - \frac{4m_g^2c^4 - 4Ap^\alpha c^\alpha(\alpha-1) - A^2\alpha^2p^{2(\alpha-1)}c^{2(\alpha-1)}}{4E^2}, \tag{A2}$$

where causality requires the numerator of the second term to be non-negative, $m_gc^2 \geq p^{\alpha-1}c^{\alpha-1}\sqrt{A(\alpha-1)p^2c^2 + (\frac{A\alpha}{2})^2}$.

An interesting case is $\alpha = 1$, which is a nonlocal theory including $p = \sqrt{p_x^2 + p_y^2 + p_z^2}$. When $\alpha = 1$, the numerator of the second term in Eq. (A2) becomes a constant and thus comparison with the usual mass case, $\frac{v_g^2}{c^2} = 1 - \frac{m_g^2c^4}{E^2}$, leads to the effective mass $m_g^{\rm eff} = \sqrt{m_g^2 - A^2/(4c^4)}$. An example of this effective mass $m_g^{\rm eff}$ has appeared in $f(R)$-gravity theories [37]. A few higher-power cases of higher derivatives, e.g., $\alpha = 3, 4$, were already discussed in Refs. [47,48].

From now on, let us consider extra dimensions. In the model of an extra dimension with $A = -\frac{\eta_{\rm ED}}{E_p^2}$ and $\alpha = 4$, the generalized dispersion relation at low energy is given by $k^2 = \omega^2 + (\eta_{\rm ED}/E_p^2)\omega^4 - m_g^2$ [49]. Under the Newtonian gauge, the response function for the breathing and longitudinal modes (57) at a frequency ω_1 is

TABLE III. The generalized dispersion relations for various gravity models. Here, E_p is the Planck energy scale, $\eta_{\rm DSR}$ is a dimensionless parameter given by the Lorentz-invariance-violating theories, $\eta_{\rm ED}$ is a positive dimensionless parameter, $\kappa_{\rm HL}$ and $\mu_{\rm HL}$ are constants of Hořava-Lifshitz theory, and $\eta_{\rm NCG}$ is a constant in the theory of noncommutative geometries.

Models	A	α	m_g	References
Doubly Special Relativity	$\eta_{\rm DSR}$	3		[50–53]
Broken-Symmetry Extra Dimension	$-\eta_{\rm ED}$	4		[49]
Hořava-Lifshitz	$\frac{\kappa_{\rm HL}^4\mu_{\rm HL}^2}{16}$	4	0	[54–58]
Noncommutative Geometries	$2\frac{\eta_{\rm NCG}}{E_p^2}$	4		[59,60]

$$S^{(b+l)}[\omega_1] \equiv S_1^{(b+l)} = F_l\left(1 + \frac{\eta_{\rm ED}}{E_p^2}\omega_1^2 - \frac{m_g^2}{\omega_1^2}\right)h_{tt}. \tag{A3}$$

Similarly, for the second frequency $\omega_2(\omega_2 \neq \omega_1)$, the difference of the response functions is

$$S_1^{(b+l)} - S_2^{(b+l)} = F_l\left(\frac{\eta_{\rm ED}}{E_p^2} + \frac{m_g^2}{\omega_1^2\omega_2^2}\right)(\omega_1^2 - \omega_2^2)h_{tt}. \tag{A4}$$

Since the right-hand side of Eq. (A4) involves the three unknown quantities $\eta_{\rm ED}/E_p^2$, m_g^2, and h_{tt}, we consider the third frequency ω_3 as different from ω_1 and ω_2 and then the expressions for $\eta_{\rm ED}/E_p^2$ and m_g^2 are given only in terms of the measured quantities, $S_i^{(b+l)}$ and ω_i $(i = 1, 2, 3)$,

$$\begin{aligned}\frac{\eta_{\rm ED}}{E_p^2} &= \omega_1^2\omega_2^2\omega_3^2\frac{(\omega_3^{-2} - \omega_2^{-2})S_1^{(b+l)} + (\omega_2^{-2} - \omega_1^{-2})S_3^{(b+l)} + (\omega_1^{-2} - \omega_3^{-2})S_2^{(b+l)}}{\omega_1^2(\omega_3^4 - \omega_2^4)S_1^{(b+l)} + \omega_3^2(\omega_2^4 - \omega_1^4)S_3^{(b+l)} + \omega_2^2(\omega_1^4 - \omega_3^4)S_2^{(b+l)}},\\ m_g^2 &= \omega_1^2\omega_2^2\omega_3^2\frac{(\omega_3^2 - \omega_2^2)S_1^{(b+l)} + (\omega_2^2 - \omega_1^2)S_3^{(b+l)} + (\omega_1^2 - \omega_3^2)S_2^{(b+l)}}{\omega_1^2(\omega_3^4 - \omega_2^4)S_1^{(b+l)} + \omega_3^2(\omega_2^4 - \omega_1^4)S_3^{(b+l)} + \omega_2^2(\omega_1^4 - \omega_3^4)S_2^{(b+l)}}.\end{aligned} \tag{A5}$$

The results of other modified gravity models are also summarized in Table III [47], with their corresponding generalized dispersion relations and references.

When extended gravity theories involving propagating massive d.o.f. are considered, the exact amplitude expressions (25), (28), and (40) can always be used to obtain the six mode polarizations of gravitational waves (two scalars, two vectors, and two tensors), irrespective of the form of their actions. Under the Newtonian gauge condition, the nonvanishing components in scalar-tensor gravity are $\delta\phi = A = -D$ and $h_+, h_\times$ [26]. The amplitudes have also been obtained for other models, e.g., Einstein-æ ther theory, tensor-vector-scalar models, etc., [61–63].

[1] D. M. Eardley, D. L. Lee, and A. P. Lightman, Gravitational-wave observations as a tool for testing relativistic gravity, Phys. Rev. D **8**, 3308 (1973).
[2] D. M. Eardley, D. L. Lee, A. P. Lightman, R. V. Wagoner, and C. M. Will, Gravitational-Wave Observations as a Tool for Testing Relativistic Gravity, Phys. Rev. Lett. **30**, 884 (1973).
[3] C. M. Will, *Theory and Experiment in Gravitational Physics* (University Press, Cambridge, England, 1993), p. 380.
[4] C. M. Will, The confrontation between general relativity and experiment, Living Rev. Relativity **17**, 4 (2014).
[5] A. Einstein, Approximative integration of the field equations of gravitation, Sitzungsber. Preuss. Akad. Wiss. Berlin (Math. Phys.) **1916**, 688 (1916); Über Gravitationswellen, Sitzungsber. Preuss. Akad. Wiss. Berlin (Math. Phys.) **1918**, 154 (1918).
[6] B. P. Abbott *et al.* (LIGO Scientific and Virgo Collaborations), Observation of Gravitational Waves from a Binary Black Hole Merger, Phys. Rev. Lett. **116**, 061102 (2016).
[7] B. P. Abbott *et al.* (LIGO Scientific and Virgo Collaborations), GW151226: Observation of Gravitational Waves from a 22-Solar-Mass Binary Black Hole Coalescence, Phys. Rev. Lett. **116**, 241103 (2016).
[8] B. P. Abbott *et al.* (LIGO Scientific and Virgo Collaborations), Binary Black Hole Mergers in the first Advanced LIGO Observing Run, Phys. Rev. X **6**, 041015 (2016).
[9] B. P. Abbott *et al.* (LIGO Scientific and Virgo Collaborations), GW170104: Observation of a 50-Solar-Mass Binary Black Hole Coalescence at Redshift 0.2, Phys. Rev. Lett. **118**, 221101 (2017).
[10] H. R. Kausar, L. Philippoz, and P. Jetzer, Gravitational Wave Polarization Modes in $f(R)$ Theories, Phys. Rev. D **93**, 124071 (2016).
[11] E. Berti *et al.*, Testing General Relativity with Present and Future Astrophysical Observations, Classical Quantum Gravity **32**, 243001 (2015).
[12] B. P. Abbott *et al.* (LIGO Scientific and Virgo Collaborations), First Search for Nontensorial Gravitational Waves from Known Pulsars, Phys. Rev. Lett. **120**, 031104 (2018).
[13] B. P. Abbott *et al.* (LIGO Scientific and Virgo Collaborations), Search for Tensor, Vector, and Scalar Polarizations in the Stochastic Gravitational-Wave Background, Phys. Rev. Lett. **120**, 201102 (2018).
[14] A. Nishizawa, A. Taruya, K. Hayama, S. Kawamura, and M. a. Sakagami, Probing non-tensorial polarizations of stochastic gravitational-wave backgrounds with ground-based laser interferometers, Phys. Rev. D **79**, 082002 (2009).
[15] M. E. S. Alves, O. D. Miranda, and J. C. N. de Araujo, Probing the f(R) formalism through gravitational wave polarizations, Phys. Lett. B **679**, 401 (2009).
[16] Y. S. Myung, Propagating degrees of freedom in $f(R)$ gravity, Adv. High Energy Phys. **2016**, 3901734 (2016).
[17] D. Bessada and O. D. Miranda, CMB polarization and theories of gravitation with massive gravitons, Classical Quantum Gravity **26**, 045005 (2009).
[18] M. E. S. Alves, O. D. Miranda, and J. C. N. de Araujo, Extra polarization states of cosmological gravitational waves in alternative theories of gravity, Classical Quantum Gravity **27**, 145010 (2010).
[19] H. Abedi and S. Capozziello, Gravitational waves in modified teleparallel theories of gravity, Eur. Phys. J. C **78**, 474 (2018).
[20] W. L. S. de Paula, O. D. Miranda, and R. M. Marinho, Polarization states of gravitational waves with a massive graviton, Classical Quantum Gravity **21**, 4595 (2004).
[21] L. Yang, C. C. Lee, and C. Q. Geng, Gravitational waves in viable $f(R)$ models, J. Cosmol. Astropart. Phys. 08 (2011) 029.
[22] A. E. Gumrukcuoglu, S. Kuroyanagi, C. Lin, S. Mukohyama, and N. Tanahashi, Gravitational wave signal from massive gravity, Classical Quantum Gravity **29**, 235026 (2012).
[23] A. Nishizawa and K. Hayama, Probing for massive stochastic gravitational-wave background with a detector network, Phys. Rev. D **88**, 064005 (2013).
[24] U. Sperhake, C. J. Moore, R. Rosca, M. Agathos, D. Gerosa, and C. D. Ott, Long-Lived Inverse Chirp Signals from Core-Collapse in Massive Scalar-Tensor Gravity, Phys. Rev. Lett. **119**, 201103 (2017).
[25] C. Corda, A Longitudinal component in massive gravitational waves arising from a biometric theory of gravity, Astropart. Phys. **28**, 247 (2007).
[26] D. Liang, Y. Gong, S. Hou, and Y. Liu, Polarizations of gravitational waves in $f(R)$ gravity, Phys. Rev. D **95**, 104034 (2017).
[27] J. C. N. de Araujo and O. D. Miranda, A Solution for galactic disks with Yukawian gravitational potential, Gen. Relativ. Gravit. **39**, 777 (2007).
[28] C. S. S. Brandao and J. C. N. Araujo, Probing Yukawian gravitational potential by numerical simulations. I. Changing N-body codes, Gen. Relativ. Gravit. **42**, 777 (2010).
[29] C. S. S. Brandao and J. C. N. de Araujo, Probing Brownstein-Moffat Gravity via Numerical Simulations, Astrophys. J. **717**, 849 (2010).
[30] C. M. Will, The Confrontation between general relativity and experiment, Living Rev. Relativity **9**, 3 (2006).
[31] V. P. Frolov and I. D. Novikov, Black Hole Physics: Basic Concepts and New Developments, *Fundamental Theories of Physics*, Vol. 96 (Springer, Switzerland, 1998).
[32] M. Isi, A. J. Weinstein, C. Mead, and M. Pitkin, Detecting Beyond-Einstein Polarizations of Continuous Gravitational Waves, Phys. Rev. D **91**, 082002 (2015).
[33] M. Visser, Mass for the graviton, Gen. Relativ. Gravit. **30**, 1717 (1998).
[34] M. E. da Silva Alves and M. Tinto, Pulsar timing sensitivities to gravitational waves from relativistic metric theories of gravity, Phys. Rev. D **83**, 123529 (2011).
[35] S. J. Chamberlin and X. Siemens, Stochastic backgrounds in alternative theories of gravity: Overlap reduction functions for pulsar timing arrays, Phys. Rev. D **85**, 082001 (2012).
[36] C. de Rham, J. T. Deskins, A. J. Tolley, and S. Y. Zhou, Graviton mass bounds, Rev. Mod. Phys. **89**, 025004 (2017).
[37] S. Lee, Constraint on reconstructed $f(R)$ gravity models from gravitational waves, Eur. Phys. J. C **78**, 449 (2018).
[38] C. Talmadge, J. P. Berthias, R. W. Hellings, and E. M. Standish, Model Independent Constraints on Possible Modifications of Newtonian Gravity, Phys. Rev. Lett. **61**, 1159 (1988).

[39] C. M. Will, Bounding the mass of the graviton using gravitational wave observations of inspiralling compact binaries, Phys. Rev. D **57**, 2061 (1998).

[40] C. M. Will, Solar system versus gravitational-wave bounds on the graviton mass, Classical Quantum Gravity **35**, 17LT01 (2018).

[41] R. Brito, V. Cardoso, and P. Pani, Massive spin-2 fields on black hole spacetimes: Instability of the Schwarzschild and Kerr solutions and bounds on the graviton mass, Phys. Rev. D **88**, 023514 (2013).

[42] A. S. Goldhaber and M. M. Nieto, Mass of the graviton, Phys. Rev. D **9**, 1119 (1974).

[43] S. Desai, Limit on graviton mass from galaxy cluster Abell 1689, Phys. Lett. B **778**, 325 (2018).

[44] S. R. Choudhury, G. C. Joshi, S. Mahajan, and B. H. J. McKellar, Probing large distance higher dimensional gravity from lensing data, Astropart. Phys. **21**, 559 (2004).

[45] L. S. Finn and P. J. Sutton, Bounding the mass of the graviton using binary pulsar observations, Phys. Rev. D **65**, 044022 (2002).

[46] B. P. Abbott *et al.* (LIGO Scientific and Virgo Collaborations), Tests of General Relativity with GW150914, Phys. Rev. Lett. **116**, 221101 (2016).

[47] S. Mirshekari, N. Yunes, and C. M. Will, Constraining Lorentz-violating, modified dispersion relations with gravitational waves, Phys. Rev. D **85**, 024041 (2012).

[48] S. Kiyota and K. Yamamoto, Constraint on modified dispersion relations for gravitational waves from gravitational Cherenkov radiation, Phys. Rev. D **92**, 104036 (2015).

[49] A. S. Sefiedgar, K. Nozari, and H. R. Sepangi, Modified dispersion relations in extra dimensions, Phys. Lett. B **696**, 119 (2011).

[50] G. Amelino-Camelia, Testable scenario for relativity with minimum length, Phys. Lett. B **510**, 255 (2001).

[51] J. Magueijo and L. Smolin, Lorentz Invariance with an Invariant Energy Scale, Phys. Rev. Lett. **88**, 190403 (2002).

[52] G. Amelino-Camelia, Doubly special relativity, Nature (London) **418**, 34 (2002).

[53] G. Amelino-Camelia, Doubly-special relativity: Facts, myths and some key open issues, Symmetry **2**, 230 (2010).

[54] P. Horava, Membranes at quantum criticality, J. High Energy Phys. 03 (2009) 020.

[55] P. Horava, Quantum gravity at a Lifshitz point, Phys. Rev. D **79**, 084008 (2009).

[56] C. Bogdanos and E. N. Saridakis, Perturbative instabilities in Horava gravity, Classical Quantum Gravity **27**, 075005 (2010).

[57] S. I. Vacaru, Modified dispersion relations in Horava-Lifshitz gravity and Finsler Brane models, Gen. Relativ. Gravit. **44**, 1015 (2012).

[58] D. Blas and H. Sanctuary, Gravitational radiation in Horava gravity, Phys. Rev. D **84**, 064004 (2011).

[59] R. Garattini and G. Mandanici, Modified dispersion relations lead to a finite zero point gravitational energy, Phys. Rev. D **83**, 084021 (2011).

[60] R. Garattini and G. Mandanici, Particle propagation and effective space-time in Gravity's rainbow, Phys. Rev. D **85**, 023507 (2012).

[61] Y. Gong, S. Hou, D. Liang, and E. Papantonopoulos, Gravitational waves in Einstein-æther and generalized T*e*V*e*S theory after GW170817, Phys. Rev. D **97**, 084040 (2018).

[62] J. Oost, M. Bhattacharjee, and A. Wang, Gravitational plane waves in Einstein-aether theory, Gen. Relativ. Gravit. **50**, 124 (2018).

[63] K. Lin, X. Zhao, C. Zhang, T. Liu, B. Wang, S. Zhang, X. Zhang, W. Zhao, T. Zhu, and A. Wang, Gravitational wave forms, polarizations, response functions and energy losses of triple systems in Einstein-aether theory, Phys. Rev. D **99**, 023010 (2019).